THE EUROPEAN
PHYSICAL JOURNAL C

Regular Article - Theoretical Physics

Black hole surrounded by the pseudo-isothermal dark matter halo

Yi Yang[1,a], **Dong Liu**[2,b], **Ali Övgün**[3,c], **Gaetano Lambiase**[4,5,d], **Zheng-Wen Long**[2,e]

[1] School of Mathematics and Statistics, Guizhou University of Finance and Economics, Guiyang 550025, China
[2] College of Physics, Guizhou University, Guiyang 550025, China
[3] Physics Department, Eastern Mediterranean University, North Cyprus via Mersin 10, Famagusta 99628, Turkey
[4] Dipartimento di Fisica "E.R Caianiello", Università degli Studi di Salerno, Via Giovanni Paolo II, 132, 84084 Fisciano, SA, Italy
[5] Istituto Nazionale di Fisica Nucleare-Gruppo Collegato di Salerno-Sezione di Napoli, Via Giovanni Paolo II, 132, 84084 Fisciano, SA, Italy

Abstract In this paper, we obtain a new spherically symmetric black hole surrounded by the pseudo-isothermal dark matter halo. Furthermore, to explore the effects of the pseudo-isothermal halo profile on a rotating black hole at the M87 galactic center, we derive a rotating black hole solution encompassed by the pseudo-isothermal halo by using the Newman-Janis method. Our investigation focuses on the impact of the pseudo-isothermal halo on the black hole event horizon, time-like and null orbits, as well as the black hole shadow. We find that as the spin parameter a increases, the interval between the inner event horizon and the outer event horizon of the rotating black hole surrounded by the pseudo-isothermal halo in M87 diminishes. This leads to the formation of an extreme black hole. The presence of dark matter, however, has minimal effect on the event horizon. Moreover, in the M87 as the spin parameter a increases, the black hole shadow deviates increasingly from a standard circle, with larger spin parameters causing more pronounced distortion relative to the standard circle. Surprisingly, we observe that the dark matter density has very little influence on the shadow of the black hole surrounded by the pseudo-isothermal halo in the M87. This study contributes to a deeper understanding of black hole structures and the role of dark matter in the universe.

Contents

1 Introduction

In 1915, Einstein put forth the groundbreaking theory of general relativity (GR) in the realm of physics, where he linked the gravitational field to the curvature of spacetime. Within this theory emerged the concept of black holes (BH), extraordinary celestial objects in the universe. Their existence was not observed directly but rather predicted based on the principles of general relativity. In 1916, Schwarzschild [1] became the first to solve the field equations of general relativity, resulting in a static spherically symmetric vacuum solution that described a non-rotating black hole with mass alone. Later, in 1963, Kerr derived a rotating, steady-state axisymmetric vacuum black hole solution [2]. However, within classical gravitational theory, a singularity exists inside the black hole [3–6].

On the other hand, the true nature of dark matter is one of the most profound mysteries in astrophysics and cosmology. The widely accepted Λ CDM model has been remarkably successful in explaining the dynamics of the large-scale Universe, suggesting that about 26.8% of our Universe is composed of dark matter, making up a significant 85% of its total mass [7]. In the early universe, the dark matter halo has been suggested as a potential factor in understanding this phe-

nomenon [8,9]. Although numerical simulations have been used to analyze the growth of black holes within dark matter halos over time, obtaining an analytical form for black holes surrounded by dark matter halo remains challenging. This difficulty arises from the unknown and uncertain behavior of dark matter particles when they interact with black holes.

The presence of a supermassive black hole at the center of a galaxy can significantly enhance the dark matter density, leading to a phenomenon called the "Spike" [10–12]. However, the Navarro-Frenk-White (NFW) density profile exhibits a "cusp" problem [13], which contradicts observations showing a rather flat density profile. Different dark matter models, such as scalar field dark matter, modified Newtonian dynamics dark matter, and warm dark matter, do not produce the "cusp" in small scales. It remains uncertain whether the "Spike" and "Cusp" manifest in the galactic center.

These challenges serve as motivation for our study, where we examine black holes (spherically symmetric and rotating) in dark matter halos under stationary conditions. By exploring the results obtained, we can investigate various dynamic processes occurring near the black hole, and the energy density of dark matter under relativistic conditions. This research seeks to shed light on the behavior of dark matter in the vicinity of black holes and provides insights into potential solutions for the observed discrepancies between theoretical predictions and observational data. One notable method for extending Schwarzschild-like black holes to Kerr-like black holes is the Newman-Janis (NJ) algorithm [14–16], which has proven to be highly suitable for this purpose. Additionally, reference [17] also contributes to the topic.

In 2019, the Event Horizon Telescope (EHT) released the first image of a black hole, capturing the shadow of the supermassive black hole M87 at the center of the Virgo elliptical galaxy [18]. Moreover, in 2022, EHT released an image of Sagittarius A*, the supermassive black hole at the center of the Milky Way [19]. The information revealed in these black hole photos has provided valuable insights into the shadow, jet, and accretion processes of black holes. As a result of these groundbreaking discoveries, the phenomenon of black hole shadows has attracted significant attention in the scientific literature. Numerous studies have been conducted to delve into this intriguing aspect [20–119]. In Ref. [120] Tang and Xu presented a spacetime metric for a rotating short-hairy black hole, and studied the influence of short-hairy on the shadow of black holes. These studies have contributed significantly to our understanding of black hole properties and their impact on the surrounding environment. In our study, we will utilize the black hole shadow to gain valuable insights into the effects of pseudo-isothermal halo (PIH) profile [121] on a rotating black hole geometry. To achieve this, we will primarily rely on the formalism developed by Xu et al. [122,123] to obtain the combined dark matter and black hole geometries. By employing these techniques, we aim to elucidate the

impact of pseudo-isothermal halo profile on a rotating black hole, specifically in the context of their observable shadows. This investigation can contribute to a deeper understanding of the interaction between black holes and dark matter and may offer valuable clues for unraveling the enigmatic nature of dark matter through astrophysical observations.

In our research, we aim to explore the shadows of rotating black holes surrounded by dark matter and analyze their unique characteristics. By doing so, we hope to provide valuable insights and directions for the experimental detection of this particular spacetime configuration. This investigation will contribute to our understanding of black hole properties and enhance our ability to interpret the observations of black hole shadows in astrophysical contexts. This work is organized as follows. In Sect. 2, we give a pure dark matter spacetime metric by considering the pseudo-isothermal halo profile, and solve the Einstein field equations to obtain the spherically symmetric BH metric surrounded by the pseudo-isothermal halo. In Sect. 3 we derive the rotating black hole surrounded by the pseudo-isothermal halo profile derived by using the Newman-Janis method. In Sect. 4, we obtain the geodesic equation by solving the Hamilton-Jacobi equation in the rotating black hole. In Sect. 5, we present the shadow images of a rotating black hole and analyze the influence of spin and dark matter parameters on the shadow. Section 6 provides our main conclusion of this work.

2 Spherically symmetric BH metric surrounded by the PIH

In this work, we study the pseudo-isothermal halo profile [121]. The dark matter density profile reads

$$\rho_{PI}(r) = \rho_0 \left[1 + \left(\frac{r}{r_0} \right)^2 \right]^{-1}. \tag{2.1}$$

where ρ_0 denotes the central halo density and r_0 denotes the halo core radius. In order to obtain a spherically symmetric black hole surrounded by dark matter, we first need to calculate the mass distribution of the dark matter halo. According to the above dark matter halo profile, we can obtain the mass profile [124])

$$M_{PI} = 4\pi \int_0^r \rho_{PI} \left(r' \right) r'^2 dr'$$
$$= 4\pi \rho_0 r_0^2 \left[r - r_0 \arctan \left(\frac{r}{r_0} \right) \right]. \tag{2.2}$$

In the spherically symmetric spacetime, we can find the tangential velocity of the test particle moving in the dark matter halo determined by the mass distribution of the dark matter

halo. Therefore, we obtain the tangential velocity (in units $G = 1, c = 1$)

$$V_{\text{PI}} = \sqrt{\frac{M_{\text{PI}}}{r}} = \sqrt{\frac{4\pi\rho_0 r_0^2 \left[r - r_0 \arctan\left(\frac{r}{r_0}\right) \right]}{r}}. \quad (2.3)$$

The spherically symmetric spacetime line elements describing pure dark matter halo can be written as (using the method introduced in Ref. [124] and later used by Xu et al. in Ref.[122])

$$ds^2 = -\mathcal{A}(r)dt^2 + \mathcal{B}(r)^{-1}dr^2 + r^2\left(d\theta^2 + \sin^2\theta d\phi^2\right), \quad (2.4)$$

where the $\mathcal{A}(r)$ represents the redshift functions, and $\mathcal{B}(r)$ represents the shape functions. The tangential velocity is closely related to the redshift function $\mathcal{A}(r)$ of the spacetime metric, which reads

$$V_{PI}^2 = r\frac{d\ln\sqrt{\mathcal{A}(r)}}{dr}. \quad (2.5)$$

It should be noted that in our work, we consider the case of $\mathcal{A}(r) = \mathcal{B}(r)$. Substituting equation (2.3) into above equation, we can obtain the analytical expression of the redshift function and the shape function in the pure dark matter metric

$$\mathcal{A}_{PI}(r) = \mathcal{B}_{PI}(r)$$
$$= \left(r_0^2 + r^2\right)^{4\pi\rho_0 r_0^2} \exp\left[\frac{8\pi\rho_0 r_0^3 \arctan\left(\frac{r}{r_0}\right)}{r}\right]. \quad (2.6)$$

Now, we will solve the Einstein field equations to obtain the spherically symmetric BH metric surrounded by the pseudo-isothermal halo. As proposed by Xu et al. [122], the Einstein field equation for the pure pseudo-isotherma dark matter spacetime need to be solved, which can be written as

$$R_{\mu\nu} - \frac{1}{2}g_{\mu\nu}R = \kappa^2 T_{\mu\nu}(\text{PIH}), \quad (2.7)$$

where $g_{\mu\nu}$ denotes the metric tensor of the pure pseudo-isothermal dark matter spacetime, $R_{\mu\nu}$ and R denotes the Ricci tensor and Ricci scalar, respectively. The energy-momentum tensor of the pure pseudo-isothermal dark matter spacetime can be written as $T^\nu{}_\mu = g^{\nu\sigma}T_{\mu\sigma} =$ diag $[-\rho, p_r, p, p]$. Therefore, we can obtain

$$\kappa^2 T^t{}_t(\text{PIH}) = \mathcal{B}_{PI}(r)\left(\frac{1}{r}\frac{\mathcal{B}'_{PI}(r)}{\mathcal{B}_{PI}(r)} + \frac{1}{r^2}\right) - \frac{1}{r^2},$$

$$\kappa^2 T^r{}_r(\text{PIH}) = \mathcal{B}_{PI}(r)\left(\frac{1}{r^2} + \frac{1}{r}\frac{\mathcal{A}'_{PI}(r)}{\mathcal{A}_{PI}(r)}\right) - \frac{1}{r^2},$$

$$\kappa^2 T^\theta{}_\theta(\text{PIH}) = \kappa^2 T^\phi{}_\phi(\text{PIH}) = \frac{1}{2}\mathcal{B}_{PI}(r)$$
$$\times \left[\frac{\mathcal{A}''_{PI}(r)\mathcal{A}_{PI}(r) - \mathcal{A}'^2_{PI}(r)}{\mathcal{A}^2_{PI}(r)} + \frac{\mathcal{A}'^2_{PI}(r)}{2\mathcal{A}^2_{PI}(r)} \right.$$
$$+ \frac{1}{r}\left(\frac{\mathcal{A}'_{PI}(r)}{\mathcal{A}_{PI}(r)} + \frac{\mathcal{B}'_{PI}(r)}{\mathcal{B}_{PI}(r)}\right)$$
$$\left. + \frac{\mathcal{A}'_{PI}(r)\mathcal{B}'_{PI}(r)}{2\mathcal{A}_{PI}(r)\mathcal{B}_{PI}(r)} \right]. \quad (2.8)$$

If consider a black hole surrounded by the PIH, the energy-momentum tensor become $T^\nu{}_\mu = T^\nu{}_\mu(\text{BH}) + T^\nu{}_\mu(\text{PIH})$. According to GR, Schwarzschild black hole is an vacuum solution, which satisfies the condition $T^\nu{}_\mu(\text{BH}) = 0$. If we consider a Schwarzschild-like BH surrounded by the PIH, we can only consider the energy-momentum tensor of the pure PIH. Therefore, we assume the black hole metric surrounded by the PIH has the following form

$$ds^2 = -[\mathcal{A}_{PI}(r) + X_1(r)]dt^2$$
$$+ \frac{1}{\mathcal{B}_{PI}(r) + X_2(r)}dr^2 + r^2\left(d\theta^2 + \sin^2\theta d\phi^2\right), \quad (2.9)$$

where $\mathcal{A}_{PI}(r)$ and $\mathcal{B}_{PI}(r)$ denote the metric coefficients of the pure PIH and the unknown functions $X_1(r)$ and $X_2(r)$ are determined by the black hole parameters and PIH parameters. As a consequence, the Einstein field equations can be cast in the form

$$R_{\mu\nu} - \frac{1}{2}g_{\mu\nu}R = \kappa^2\left[T_{\mu\nu}(\text{BH}) + T_{\mu\nu}(\text{PIH})\right]. \quad (2.10)$$

Substituting the new black hole metric (2.9) into the above Einstein field equation, we can obtain

$$[\mathcal{B}_{PI}(r) + X_2(r)]\left[\frac{1}{r^2} + \frac{1}{r}\frac{\mathcal{B}'_{PI}(r) + X'_2(r)}{\mathcal{B}_{PI}(r) + X_2(r)}\right]$$
$$= \mathcal{B}_{PI}(r)\left[\frac{1}{r^2} + \frac{1}{r}\frac{\mathcal{B}'_{PI}(r)}{\mathcal{B}_{PI}(r)}\right], \quad (2.11a)$$

$$[\mathcal{B}_{PI}(r) + X_2(r)]\left[\frac{1}{r^2} + \frac{1}{r}\frac{\mathcal{A}'_{PI}(r) + X'_1(r)}{\mathcal{A}_{PI}(r) + X_1(r)}\right]$$
$$= \mathcal{B}_{PI}(r)\left[\frac{1}{r^2} + \frac{1}{r}\frac{\mathcal{A}'_{PI}(r)}{\mathcal{A}_{PI}(r)}\right]. \quad (2.11b)$$

Using the Schwarzschild black hole as the boundary condition, we can obtain the analytical solution of the above two

differential equations

$$X_2(r) = -\frac{2M}{r},$$

$$X_1(r) = \exp\left\{ \int \frac{\mathcal{B}_{PI}(r)}{\mathcal{B}_{PI}(r) + X_2(r)} \left[\frac{1}{r} + \frac{\mathcal{A}'_{PI}(r)}{\mathcal{A}_{PI}(r)} \right] \right.$$

$$\left. dr - \frac{1}{r}dr \right\} - \mathcal{A}_{PI}(r). \tag{2.12}$$

For the pseudo-isothermal halo, if $\mathcal{A}_{PI}(r) = \mathcal{B}_{PI}(r)$, one can find that $X_1(r) = X_2(r) = -2M/r$. The black hole surrounded by the pseudo-isothermal halo can be hence written as

$$ds^2 = -Q_1(r)dt^2 + \frac{1}{Q_2(r)}dr^2 + \mathcal{R}(r)\left(d\theta^2 + \sin^2\theta d\phi^2 \right), \tag{2.13}$$

where $\mathcal{R}(r) = r^2$, and $Q_1 = X_1(r) + \mathcal{A}_{PI}(r) = Q_2 = X_2(r) + \mathcal{B}_{PI}(r)$, whose explicit expressions are

$$Q_1(r) = Q_2(r)$$

$$= \left(r_0^2 + r^2\right)^{4\pi\rho_0 r_0^2} \exp\left[\frac{8\pi\rho_0 r_0^3 \arctan\left(\frac{r}{r_0}\right)}{r} \right]$$

$$- \frac{2M}{r}. \tag{2.14}$$

3 Rotating black hole surrounded by the pseudo-isothermal halo

The black hole photos taken by EHT and the detection of gravitational wave events indicate that the black holes in the actual universe are Kerr-like black holes, i.e., they usually have spins. Therefore, we will introduce spin into the spherically symmetric black hole spacetime. To achieve this, we will use the Newman-Janis algorithm, which allows us to introduce the spin into the black hole surrounded by the pseudo-isothermal halo. In the NJ method, in order to obtain the spacetime metric of a rotating black hole surrounded by the pseudo-isothermal halo, it is necessary to transform the spherically symmetric metric from Boyer–Lindquist to Eddington–Finkelstein coordinates. The relationship between the Boyer–Lindquist coordinates (t, r, θ, ϕ) and the advanced null coordinate (u, r, θ, ϕ) is

$$du = dt - dr_* = dt - \frac{dr}{Q_1(r)}. \tag{3.1}$$

The contravariant metric tensor $g^{\mu\nu}$ for a spherically symmetric metric can be given by the four basis vectors $(l^\mu, n^\mu, m^\mu, \bar{m}^\mu)$

$$g^{\mu\nu} = -l^\mu n^\nu - l^\nu n^\mu + m^\mu \bar{m}^\nu + m^\nu \bar{m}^\mu, \tag{3.2}$$

where the four basis vectors satisfy the orthogonality conditions and the modulus of the basis vector is one, i.e.

$$l^\mu l_\mu = n^\mu n_\mu = m^\mu m_\mu = \bar{m}^\mu \bar{m}_\mu = 0,$$
$$l^\mu m_\mu = l^\mu \bar{m}_\mu = n^\mu m_\mu = n^\mu \bar{m}_\mu = 0, \tag{3.3}$$
$$-l^\mu n_\mu = m^\mu \bar{m}_\mu = 1.$$

For the metric of a rotating black hole surrounded by the pseudo-isothermal halo, the basis vectors are

$$l^\mu = \delta_r^\mu,$$

$$n^\mu = \sqrt{\frac{Q_2(r)}{Q_1(r)}}\delta_u^\mu - \frac{Q_1(r)}{2}\delta_r^\mu,$$

$$m^\mu = \frac{1}{\sqrt{2\mathcal{R}(r)}}\delta_\theta^\mu + \frac{i}{\sqrt{2\mathcal{R}(r)}\sin\theta}\delta_\phi^\mu, \tag{3.4}$$

$$\bar{m}^\mu = \frac{1}{\sqrt{2\mathcal{R}(r)}}\delta_\theta^\mu - \frac{i}{\sqrt{2\mathcal{R}(r)}\sin\theta}\delta_\phi^\mu.$$

According to the NJ method, the spacetime coordinates for different observers satisfy the following complex transformation

$$u \to u - ia\cos\theta, \quad r \to r - ia\cos\theta. \tag{3.5}$$

Using this transformation, the metric coefficient will include spin, i.e., the metric coefficient becomes a function of (r, θ, a). According to the above complex transformation, the metric functions become: $Q_1(r) \to \mathcal{W}(r, \theta, a)$, $Q_2(r) \to \mathcal{Z}(r, \theta, a)$ and $\mathcal{R}(r) \to \Sigma(r, \theta, a)$. After considering this change, the null tetrad become

$$l^\mu = \delta_r^\mu,$$

$$n^\mu = \sqrt{\frac{\mathcal{Z}}{\mathcal{W}}}\delta_u^\mu - \frac{\mathcal{Z}}{2}\delta_r^\mu,$$

$$m^\mu = \frac{1}{\sqrt{2\Sigma}}\left[\delta_\theta^\mu + ia\sin\theta\left(\delta_u^\mu - \delta_r^\mu \right) + \frac{i}{\sin\theta}\delta_\phi^\mu \right], \tag{3.6}$$

$$\bar{m}^\mu = \frac{1}{\sqrt{2\Sigma}}\left[\delta_\theta^\mu - ia\sin\theta\left(\delta_u^\mu - \delta_r^\mu \right) - \frac{i}{\sin\theta}\delta_\phi^\mu \right].$$

Therefore, according to these null tetrads, the contravariant metric tensor of the rotating black hole surrounded by the pseudo-isothermal halo can be written as

$$g^{\mu\nu} = \begin{pmatrix} \frac{a^2\sin^2\theta}{\Sigma} & -\sqrt{\frac{\mathcal{Z}}{\mathcal{W}}} - \frac{a^2\sin^2\theta}{\Sigma} & 0 & \frac{a}{\Sigma} \\ -\sqrt{\frac{\mathcal{Z}}{\mathcal{W}}} - \frac{a^2\sin^2\theta}{\Sigma} & \mathcal{Z} + \frac{a^2\sin^2\theta}{\Sigma} & 0 & -\frac{a}{\Sigma} \\ 0 & 0 & \frac{1}{\Sigma} & 0 \\ \frac{a}{\Sigma} & -\frac{a}{\Sigma} & 0 & \frac{1}{\Sigma\sin^2\theta} \end{pmatrix}. \tag{3.7}$$

Moreover, the covariant non-zero metric tensor components are given by

$$
g_{uu} = -\mathcal{W}, \quad g_{ur} = -\sqrt{\frac{\mathcal{W}}{\mathcal{Z}}},
$$
$$
g_{u\phi} = a \sin^2 \theta \left(\mathcal{W} - \sqrt{\frac{\mathcal{Z}}{\mathcal{W}}} \right),
$$
$$
g_{r\phi} = a \sin^2 \theta \sqrt{\frac{\mathcal{W}}{\mathcal{Z}}}, \quad g_{\theta\theta} = \Sigma,
$$
$$
g_{\phi\phi} = \Sigma \sin^2 \theta + a^2 \left(2\sqrt{\frac{\mathcal{Z}}{\mathcal{W}}} - \mathcal{W} \right) \sin^4 \theta. \tag{3.8}
$$

Then, we can obtain the rotating black hole surrounded by the pseudo-isothermal halo in Eddington-Finkelstein coordinates

$$
ds^2 = -\mathcal{W} du^2 - 2\sqrt{\frac{\mathcal{W}}{\mathcal{Z}}} du dr
$$
$$
+ 2a \sin^2 \theta \left(\mathcal{W} - \sqrt{\frac{\mathcal{Z}}{\mathcal{W}}} \right) du d\phi
$$
$$
+ 2a \sin^2 \theta \sqrt{\frac{\mathcal{W}}{\mathcal{Z}}} dr d\phi + \Sigma d\theta^2
$$
$$
+ \left[\Sigma \sin^2 \theta + a^2 \left(2\sqrt{\frac{\mathcal{Z}}{\mathcal{W}}} - \mathcal{W} \right) \sin^4 \theta \right] d\phi^2. \tag{3.9}
$$

One significant challenge in describing black holes is the presence of coordinate singularities, particularly at the event horizon. The Boyer–Lindquist coordinates are chosen to avoid singularities at the event horizon, making them regular there, which is crucial for understanding the physical properties of the black hole, especially when studying the behavior of objects and light near the horizon. Moreover, The Boyer–Lindquist coordinates are manifestly covariant under coordinate transformations, which means that the mathematical expressions for physical quantities maintain the same form regardless of the chosen coordinates. The number of non-zero off-diagonal components of the metric is minimal in Boyer–Lindquist coordinates [125]. Therefore, transforming the Eddington–Finkelstein coordinates back to Boyer–Lindquist coordinates is necessary. To this purpose, we use the following coordinate transformation

$$
du = dt + \mathcal{T}_1(r) dr, \quad d\phi = d\phi' + \mathcal{T}_2(r) dr, \tag{3.10}
$$

where the $\mathcal{T}_1(r)$ and $\mathcal{T}_2(r)$ take the form [126]

$$
\mathcal{T}_1(r) = -\frac{\mathcal{U}(r) + a^2}{Q_1(r) Q_2(r) + a^2}, \quad \mathcal{T}_2(r) = -\frac{a}{Q_1(r) Q_2(r) + a^2},
$$

$$\tag{3.11}$$

with

$$
\mathcal{U}(r) = \sqrt{\frac{Q_2(r)}{Q_1(r)}} \mathcal{R}(r), \tag{3.12}
$$

and

$$
\mathcal{W}(r, \theta) = \frac{\left[Q_2(r) \mathcal{R}(r) + a^2 \cos^2 \theta \right] \Sigma}{\left[\mathcal{U}(r) + a^2 \cos^2 \theta \right]^2},
$$
$$
\mathcal{Z}(r, \theta) = \frac{Q_2(r) \mathcal{R}(r) + a^2 \cos^2 \theta}{\Sigma}. \tag{3.13}
$$

Therefore, the spacetime metric of the rotating black hole surrounded by the pseudo-isothermal halo can be given by

$$
ds^2 = -\left(1 - \frac{r^2 - \mathcal{A}_{PI}(r) r^2 + 2Mr}{\Sigma} \right) dt^2
$$
$$
+ \frac{\Sigma}{\Delta} dr^2 - 2a \sin^2 \theta \left(\frac{r^2 - \mathcal{A}_{PI}(r) r^2 + 2Mr}{\Sigma} \right) dt d\phi
$$
$$
+ \Sigma d\theta^2 + \Big((a^2 + r^2) \sin^2 \theta
$$
$$
+ \frac{a^2 \sin^4 \theta (r^2 - \mathcal{A}_{PI}(r) r^2 + 2Mr)}{\Sigma} \Big) d\phi^2, \tag{3.14}
$$

where Σ and Δ are defined by

$$
\Sigma = r^2 + a^2 \cos^2 \theta, \tag{3.15a}
$$
$$
\Delta = \left(r_0^2 + r^2 \right)^{4\pi\rho_0 r_0^2} \exp \left[\frac{8\pi\rho_0 r_0^3 \arctan \left(\frac{r}{r_0} \right)}{r} \right]
$$
$$
- 2Mr + a^2. \tag{3.15b}
$$

For $a = 0$, the rotating black hole surrounded by the pseudo-isothermal halo degenerates into the non-rotating black hole surrounded by the pseudo-isothermal halo, while for $\rho_0 = 0$, the rotating black hole surrounded by the pseudo-isothermal halo degenerates into the Kerr black hole. The Schwarzschild black hole metric is recovered for $a = 0$, $\rho_0 = 0$.

The Kerr black hole in general relativity usually has two event horizons, the outer event horizon and the inner event horizon. For the rotating black hole surrounded by the pseudo-isothermal halo we obtained in the previous section, it is worth studying whether its event horizon is affected by dark matter. For a Kerr-like black hole, the event horizon is obtained by solving the equation $\Delta(r) = 0$. For the rotating black hole surrounded by the pseudo-isothermal halo, the
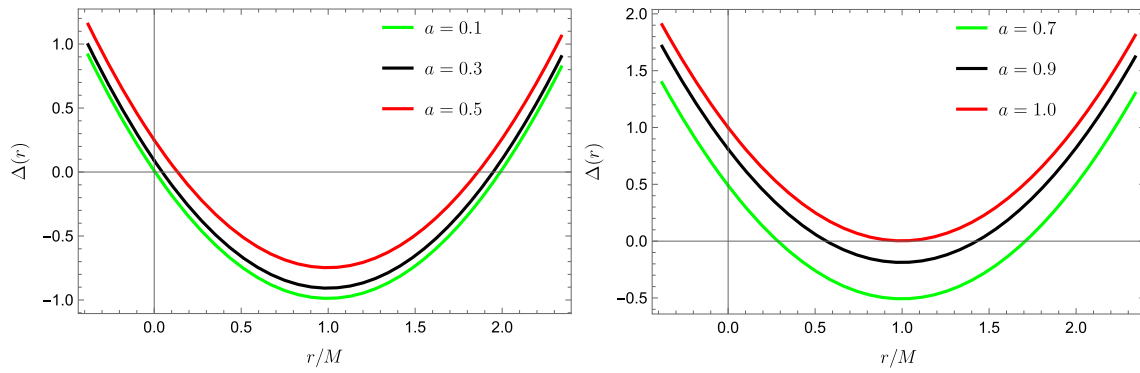
Fig. 1 $\Delta(r)$ as the function of r (see Eq. (3.15b)), with $\rho_0 = 6.9 \times 10^6 M_\odot/kpc^3$, $r_0 = 91.2$kpc. The three curves in the left panel correspond to the results of $a = 0.1$, $a = 0.3$ and $a = 0.5$, respectively. The three curves in the right panel correspond to the results of $a = 0.7$, $a = 0.9$ and $a = 1$, respectively
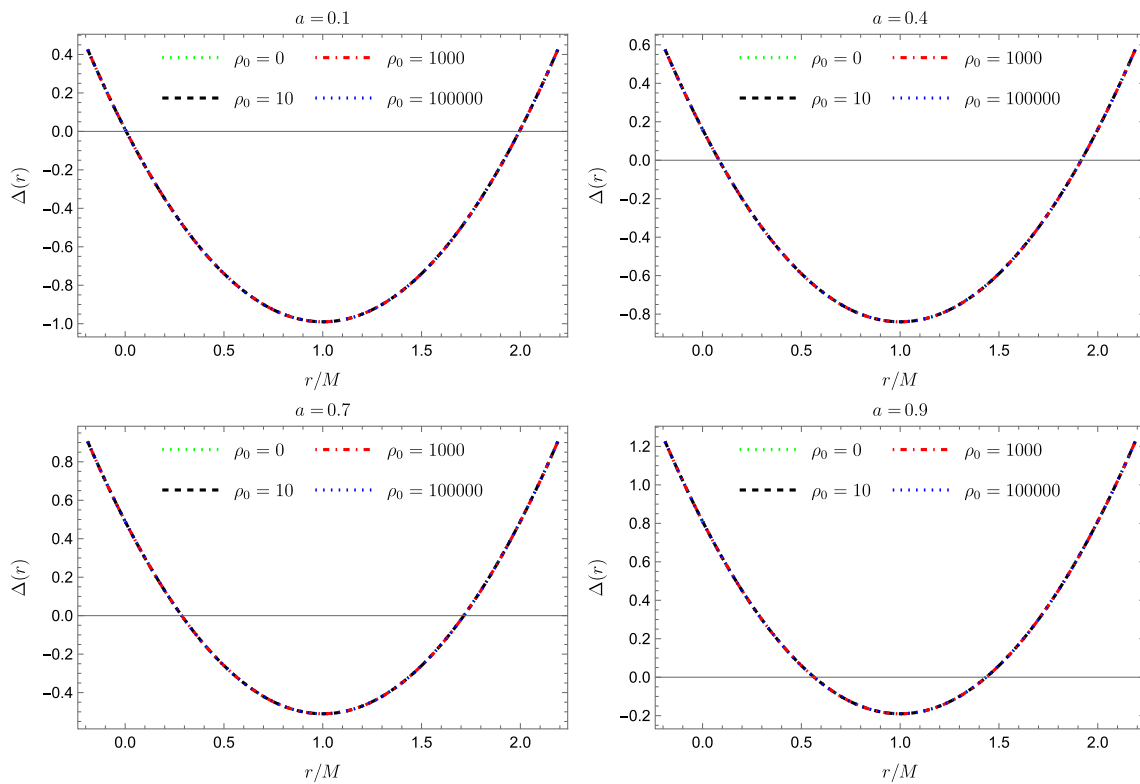

Fig. 2 $\Delta(r)$ as the function of r (see Eq. (3.15b)), with $r_0 = 91.2$kpc. From left to right and from top to bottom the values of a are $a = 0.1$, $a = 0.4$, $a = 0.7$ and $a = 0.9$ result, respectively. Here we study the effect of different dark matter densities on the event horizon. The green curve represents $\rho_0 = 0M_\odot/kpc^3$, the black curve represents $\rho_0 = 10M_\odot/kpc^3$, the red curve represents $\rho_0 = 1000M_\odot/kpc^3$, and the blue curve represents $\rho_0 = 100,000M_\odot/kpc^3$

event horizon is obtained by solving the following equation

$$\Delta(r) = \left(r_0^2 + r^2\right)^{4\pi\rho_0 r_0^2} \exp\left[\frac{8\pi\rho_0 r_0^3 \arctan\left(\frac{r}{r_0}\right)}{r}\right]$$

$$-2Mr + a^2 = 0. \tag{3.16}$$

For this equation, we cannot give an analytical solution, so we use numerical analysis to study the event horizon structure. In Figs. 1 and 2, we give $\Delta(r)$ as the function of r. From Figs. 1 and 2, we can see that the rotating black hole surrounded by the pseudo-isothermal halo still has a inner event horizon and event horizon. From Fig. 1, one can find that as the spin parameter a increases, the inter-

val between the inner event horizon and the outer event horizon becomes smaller and smaller, and the rotating dark matter black hole finally becomes an extreme black hole. In Fig. 2, the green curve represents $\rho_0 = 0 M_\odot/kpc^3$, the black curve represents $\rho_0 = 10 M_\odot/kpc^3$, the red curve represents $\rho_0 = 1000 M_\odot/kpc^3$, and the blue curve represents $\rho_0 = 100,000 M_\odot/kpc^3$. From Fig. 2, one can see that the existence of dark matter has a tiny effect on the event horizon.

4 Geodesics around the rotating black hole surrounded by the pseudo-isothermal dark matter halo

It is well known that there are two main situations for the motion of photons propagating in a gravitational background of a black hole: (i) photons with smaller impact parameters will fall into the black hole and cannot be detected; (ii) photons with impact parameter greater than a certain critical value, and they can be detected by the observer. In this section, we will study the geodesic equation of the rotating spacetime surrounded by the pseudo-isothermal dark matter halo. Our main concern is the Hamilton–Jacobi equation, which is defined as

$$\frac{\partial \mathcal{I}}{\partial \lambda} = -\mathcal{H}, \tag{4.1}$$

where $\mathcal{I}$ denotes the Jacobi action, and λ denotes the geodesic affine parameter. Furthermore, the Hamiltonian $\mathcal{H}$ reads

$$\mathcal{H} = \frac{1}{2} g^{\mu\nu} \frac{\partial \mathcal{I}}{\partial x^\mu} \frac{\partial \mathcal{I}}{\partial x^\nu}. \tag{4.2}$$

For the rotational black hole surrounded by the pseudo-isothermal halo, the Hamilton–Jacobi equation is given by

$$\frac{\partial \mathcal{I}}{\partial \lambda} = -\frac{1}{2} g^{\mu\nu} \frac{\partial \mathcal{I}}{\partial x^\mu} \frac{\partial \mathcal{I}}{\partial x^\nu}. \tag{4.3}$$

By using the method of the separation of variables, the action $\mathcal{I}$ assumes the form

$$\mathcal{I} = \frac{1}{2} \mu^2 \lambda - Et + L\phi + S_r(r) + S_\theta(\theta) \tag{4.4}$$

where μ is the mass of the particle. E and L are the conserved quantities in the motion of photons along the geodesic. Moreover, $S_r(r)$ and $S_\theta(\theta)$ denote the radial and angular functions, respectively. Substituting the action $\mathcal{I}$ into Eq. (4.3), and using the functions $\{S_r(r), S_\theta(\theta)\}$ and the conserved quanti-

ties $\{E, L\}$, we obtain

$$\Sigma \frac{dt}{d\lambda} = E \left[\frac{(a^2 + r^2)(a^2 + r^2 - aL/E)}{\Delta(r)} - a \left(a \sin^2 \theta - L/E \right) \right],$$

$$\Sigma \frac{dr}{d\lambda} = \sqrt{R(r)},$$

$$\Sigma \frac{d\theta}{d\lambda} = \sqrt{\Theta(\theta)},$$

$$\Sigma \frac{d\phi}{d\lambda} = E \left[\frac{a(a^2 + r^2 - aL/E)}{\Delta(r)} - \left(a - L/E \csc^2 \theta \right) \right], \tag{4.5}$$

where $R(r)$ and $\Theta(\theta)$ are defined as

$$R(r) = \left[E(r^2 + a^2) - aL \right]^2 - \Delta(r) \left[\mathcal{Q} + (aE - L)^2 + \mu^2 r^2 \right], \tag{4.6}$$

$$\Theta(\theta) = \mathcal{Q} - a^2(\mu^2 - E^2) \cos^2 \theta - L^2 \cot^2 \theta,$$

and $\mathcal{Q}$ represents the Carter constant [127], which is an integral constant introduced by Carter. The Eqs. (4.5) and (4.6) are complete time-like geodesics and null geodesics equations. When $\mu = 1$ they describe the motion of time-like particles, and when $\mu = 0$ they describe the motion of null particles. For the black hole shadow, we consider null geodesics, i.e. $\mu = 0$. Note that $R(r)$ and $\Theta(\theta)$ must be greater than 0, i.e.

$$\frac{R(r)}{E^2} = [r^2 + a^2 - a\xi]^2 - \Delta(r) \left[\eta + (\xi - a)^2 \right] \geq 0, \tag{4.7}$$

$$\frac{\Theta(\theta)}{E^2} = \eta + (\xi - a)^2 - \left(\frac{\xi}{\sin \theta} - a \sin \theta \right)^2 \geq 0. \tag{4.8}$$

where the impact parameters are defined as

$$\xi = L/E, \quad \eta = \mathcal{Q}/E^2. \tag{4.9}$$

The condition satisfied by the stable motion orbit region of the photon is $R''(r) > 0$, and the condition satisfied by the unstable motion orbit region of the photon is $R''(r) < 0$. The critical orbit between the stable orbit and the unstable orbit satisfies the condition

$$R(r)|_{r_{ph}} = 0, \quad \frac{dR(r)}{dr}\bigg|_{r_{ph}} = 0, \tag{4.10}$$

where r_{ph} denotes the radius of the photo-sphere. According to the above conditions, the critical impact parameters can
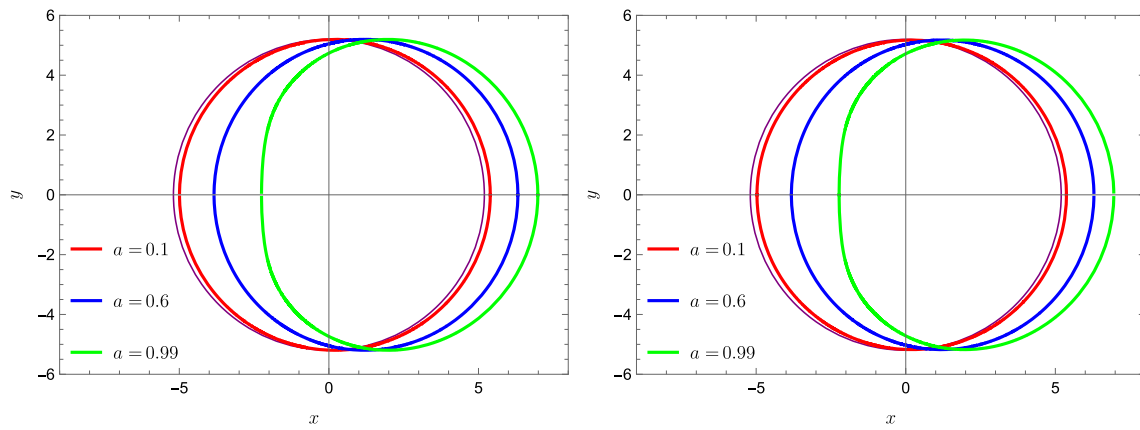
Fig. 3 The shadow of the black hole as the spin parameter a varies. The left panel is the shadow of the Kerr black hole when the dark matter density ρ_0 is zero. The right panel is the shadow of a rotating black hole surrounded by the pseudo-isothermal dark matter halo, where the parameters are set to $M = 1$, $\rho_0 = 6.9 \times 10^6 M_{\odot}/kpc^3$, $r_0 = 91.2$ kpc. Moreover, the purple solid line is the shadow of the Schwarzschild black hole

be written as

$$\xi = \frac{a^2 + r^2}{a} - \frac{4r\left[a^2 + r^2 \mathcal{A}_{PI}(r) - 2Mr\right]}{a\left[r^2 \mathcal{A}'_{PI}(r) + 2r\mathcal{A}_{PI}(r) - 2M\right]}, \quad (4.11)$$

and

$$\eta = \frac{r^5\left[8a^2 \mathcal{A}'_{PI}(r) + \left(2\mathcal{A}_{PI}(r) - r\mathcal{A}'_{PI}(r)\right)\left(r^2 \mathcal{A}'_{PI}(r) - 2r\mathcal{A}_{PI}(r) + 12M\right)\right] + 4Mr^3\left(4a^2 - 9Mr\right)}{a^2\left[r^2 \mathcal{A}'_{PI}(r) + 2r\mathcal{A}_{PI}(r) - 2M\right]^2}, \quad (4.12)$$

where $\mathcal{A}_{PI}(r)$ is given by the Eq. (2.6), and $\mathcal{A}'_{PI}(r)$ denotes the derivation $\frac{d\mathcal{A}_{PI}(r)}{dr}$.

5 The shadow shape of rotating BH surrounded by the pseudo-isothermal halo

Through the research in the previous section we obtained the geodesics of photons, and based on these results we can calculate the motion of photons detected in a rotating black hole surrounded by the pseudo-isothermal halo for any observer. To draw shadow images, people usually use celestial coordinates (x and y), which is a two-dimensional coordinate system. For an observer at the position (r, θ), the celestial coordinates are defined as [128,129]

$$\begin{aligned} x &= \lim_{r \to \infty}\left(-r^2 \sin\theta \frac{d\phi}{dr}\right), \\ y &= \lim_{r \to \infty}\left(r^2 \frac{d\theta}{dr}\right). \end{aligned} \quad (5.1)$$

where r represents the space distance from the observer to the rotating black hole surrounded by the pseudo-isothermal halo, while θ represents the angle between the straight line determined by the observer and the center of the black hole, and the rotation axis of the black hole. The motion of photons is described by $d\phi/dt$ and $d\theta/dt$. For asymptotically flat black hole metrics, the celestial coordinates can be simplified as

$$x = -\frac{\xi}{\sin\theta}, \quad (5.2)$$

and

$$y = \pm\sqrt{\eta + a^2 \cos^2\theta - \xi^2 \cot^2\theta}. \quad (5.3)$$

In our work, we consider that the observer is located on the equatorial plane of the rotating black hole surrounded by the pseudo-isothermal halo, i.e., $\theta = \pi/2$. Therefore, the celestial coordinates can be written as $x = -\xi$, and $y = \pm\sqrt{\eta}$.

Using x and y we can present the shadow image of the rotating black hole surrounded by the pseudo-isothermal halo. It allows us to study the influence of the presence of dark matter on the black hole through the image of the shadow. In Fig. 3 we investigate the effect of the spin parameter a on the shadow of the rotating black hole surrounded by the pseudo-isothermal halo. The left panel of Fig. 3 is the shadow of the Kerr black hole when the dark matter density ρ_0 is zero. The right panel of Fig. 3 is the
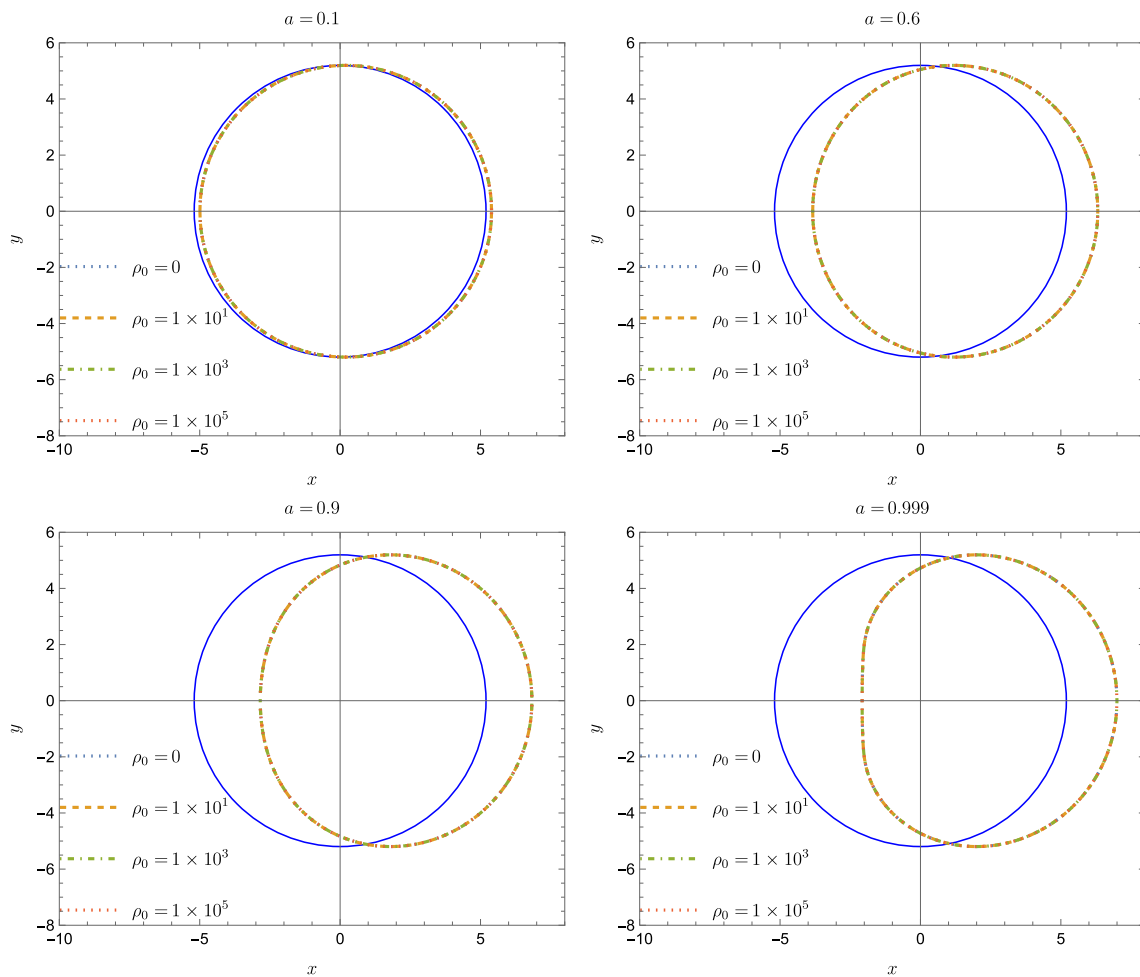
Fig. 4 The shadow of the black hole as the different dark matter densities ρ_0 varies. From left to right and from top to bottom are different spin parameters $a = 0.1$, $a = 0.6$, $a = 0.9$, and $a = 0.999$. The blue solid line is the shadow of the Schwarzschild black hole, and $\rho_0 = 0$ corresponds to the shadow of the Kerr black hole. The other parameters are set to $M = 1$, $r_0 = 91.2$ kpc

shadow of rotating black hole surrounded by the pseudo-isothermal dark matter halo, where the parameters are set to $M = 1$, $\rho_0 = 6.9 \times 10^6 M_\odot / kpc^3$, $r_0 = 91.2$ kpc. Moreover, the purple solid line is the shadow of the Schwarzschild black hole, which is a standard circle. From Fig. 3, one can find that as the spin parameter a increases, the shadow of the rotating black hole surrounded by the pseudo-isothermal halo gradually deviates from a standard circle. The left half of the shadow image is gradually distorted, while the right half of the shadow is still a standard semicircle. Furthermore, the shadow of the rotating black hole surrounded by the pseudo-isothermal halo is very similar to that of the Kerr black hole.

In Fig. 4 we study the effect of dark matter density on the black hole shadow. From left to right and from top to bottom in Fig. 4 are different spin parameters $a = 0.1$, $a = 0.6$, $a = 0.9$, and $a = 0.999$. The blue solid line is the shadow of the Schwarzschild black hole, and $\rho_0 = 0$ corresponds to the shadow of the kerr black hole. The other parameters are set

to $M = 1$, $r_0 = 91.2$ kpc. From Fig. 4, one can find that the dark matter density has a very little influence on the black hole shadow.

6 Conclusion

The abundance of dark matter in our universe is substantial, leading us to consider a black hole enveloped by dark matter. Our research involves a link of the spherically symmetric Schwarzschild black hole with the pseudo-isothermal halo profile, resulting in a spherically symmetric black hole metric surrounded by dark matter. Observations of black hole photos taken by EHT and gravitational wave events have shown that black holes likely possess spin. To account for this, we employ the Newman-Janis method to derive a rotating black hole surrounded by the pseudo-isothermal halo,

which brings us closer to a black hole solution akin to those in the real universe.

Our investigation delves into the effects of the pseudo-isothermal halo profile on the black hole event horizon, time-like and null orbits, and the shadow of the rotating black hole. We find that as the spin parameter a increases, the interval between the inner event horizon and the outer event horizon of the rotating black hole surrounded by the pseudo-isothermal halo in M87 diminishes, yielding eventually the formation of an extreme black hole. Moreover, our research reveals that the presence of dark matter has minimal impact on the event horizon. However, as the spin parameter a increases, the shadow of the rotating black hole surrounded by the pseudo-isothermal halo in M87 deviates increasingly from a standard circle, with larger spin parameters causing more pronounced distortion relative to the standard circle.

Interestingly, the dark matter density appears to have very little influence on the black hole shadow. The shadows we observe suggest that dark matter density does not significantly affect the black hole shadow, even with varying densities. The observed shadow images closely resemble those of the Kerr black hole, even in the presence of dark matter, indicating that dark matter has minimal influence on the shadow. This raises the question of whether gravitational waves emitted by the rotating black hole surrounded by the pseudo-isothermal halo would also be challenging to distinguish from those of the Kerr black hole. A relatively important stage in the gravitational wave signal is the quasinormal mode, and it carries the unique characteristics of the background spacetime. Therefore, it is necessary to further study the quasinormal mode of these black holes surrounded by the pseudo-isothermal halo. We intend to explore the quasinormal mode of the rotating black hole surrounded by the pseudo-isothermal halo in M87, which will be presented in a future work. The insights gained from gravitational waves and shadow observations hold the potential to guide experimental detection efforts.

Data availability statement This manuscript has no associated data or the data will not be deposited. [Authors' comment: All the data of this paper are shown in the manuscript. There is no data need to be deposited.]

References

1. K. Schwarzschild, On the gravitational field of a mass point according to Einstein's theory, *Sitzungsber. Preuss. Akad. Wiss. Berlin (Math. Phys.)***1916**, 189 (1916). arXiv:physics/9905030

2. R.P. Kerr, Gravitational field of a spinning mass as an example of algebraically special metrics. Phys. Rev. Lett. (1963). https://doi.org/10.1103/PhysRevLett.11.23711237

3. P.S. Joshi, Gravitational collapse: The Story so far. Pramana **55**, 529 (2000). https://doi.org/10.1007/s12043-000-0164-4. arXiv:gr-qc/0006101

4. N. Tsukamoto, Gravitational lensing in the Simpson-Visser black-bounce spacetime in a strong deflection limit. Phys. Rev. D **103**, 024033 (2021). https://doi.org/10.1103/PhysRevD.103.024033. arXiv:2011.03932

5. J. Barrientos, A. Cisterna, N. Mora, A. Viganò, AdS-Taub-NUT spacetimes and exact black bounces with scalar hair. Phys. Rev. D **106**, 024038 (2022). https://doi.org/10.1103/PhysRevD.106.024038. arXiv:2202.06706

6. A. Övgün, Weak Deflection Angle of Black-bounce Traversable Wormholes Using Gauss-Bonnet Theorem in the Dark Matter Medium. Turk. J. Phys. **44**, 465 (2020). https://doi.org/10.20944/preprints202008.0512.v1. arXiv:2011.04423

7. Planck collaboration, Planck 2013 results. I. Overview of products and scientific results. Astron. Astrophys.**571**, A1 (2014). https://doi.org/10.1051/0004-6361/201321529. arXiv:1303.5062

8. S. Balberg, S.L. Shapiro, S. Inagaki, Selfinteracting dark matter halos and the gravothermal catastrophe. Astrophys. J. **568**, 475 (2002). https://doi.org/10.1086/339038. arXiv:astro-ph/0110561

9. S. Balberg, S.L. Shapiro, S. Inagaki, Selfinteracting dark matter halos and the gravothermal catastrophe. Astrophys. J. **568**, 475 (2002). https://doi.org/10.1086/339038. arXiv:astro-ph/0110561

10. L. Sadeghian, F. Ferrer, C.M. Will, Dark matter distributions around massive black holes: A general relativistic analysis. Phys. Rev. D **88**, 063522 (2013). https://doi.org/10.1103/PhysRevD.88.063522. arXiv:1305.2619

11. L. Sadeghian, F. Ferrer, C.M. Will, Dark matter distributions around massive black holes: A general relativistic analysis. Phys. Rev. D **88**, 063522 (2013). https://doi.org/10.1103/PhysRevD.88.063522. arXiv:1305.2619

12. B.D. Fields, S.L. Shapiro, J. Shelton, Galactic center gamma-ray excess from dark matter annihilation: Is there a black hole spike? Phys. Rev. Lett. **113**, 151302 (2014). https://doi.org/10.1103/PhysRevLett.113.151302. arXiv:1406.4856

13. W.J.G. de Blok, The core-cusp problem. Adv. Astron. **2010** 1 (2010). https://doi.org/10.1155/2010/789293

14. E.T. Newman, A.I. Janis, Note on the Kerr spinning particle metric. J. Math. Phys. **6**, 915 (1965). https://doi.org/10.1063/1.1704350

15. M. Azreg-Ainou, Regular and conformal regular cores for static and rotating solutions. Phys. Lett. B **730**, 95 (2014). https://doi.org/10.1016/j.physletb.2014.01.041. [arXiv:1401.0787]

16. M. Azreg-Aïnou, Generating rotating regular black hole solutions without complexification. Phys. Rev. D **90**, 064041 (2014). https://doi.org/10.1103/PhysRevD.90.064041. arXiv:1405.2569

17. R. Shaikh, K. Pal, K. Pal, T. Sarkar, Constraining alternatives to the Kerr black hole. Mon. Not. Roy. Astron. Soc. **506**, 1229 (2021). https://doi.org/10.1093/mnras/stab1779. [arXiv:2102.04299]

18. Event Horizon Telescope collaboration, First M87 Event Horizon Telescope Results. I. The Shadow of the Supermassive Black Hole. Astrophys. J. Lett. **875**, L1 (2019). https://doi.org/10.3847/2041-8213/ab0ec7. arXiv:1906.11238

19. Event Horizon Telescope collaboration, First Sagittarius A* Event Horizon Telescope Results. II. EHT and Multiwavelength Observations, Data Processing, and Calibration. Astrophys. J. Lett. **930**, L13 (2022). https://doi.org/10.3847/2041-8213/ac6675

20. S. Capozziello, S. Zare, H. Hassanabadi, Testing bumblebee gravity with global monopoles in a dark matter spike by EHT observations from M87 and Sgr A. arXiv:2311.12896

21. J.C. Feng, S. Chakraborty, V. Cardoso, Shielding a charged black hole. Phys. Rev. D **107**, 044050 (2023). https://doi.org/10.1103/PhysRevD.107.044050. arXiv:2211.05261

22. I. Banerjee, S. Chakraborty, S. SenGupta, Silhouette of M87*: A New Window to Peek into the World of Hidden Dimensions. Phys. Rev. D **101**, 041301 (2020). https://doi.org/10.1103/PhysRevD.101.041301. arXiv:1909.09385

23. I. Banerjee, S. Chakraborty, S. SenGupta, Hunting extra dimensions in the shadow of Sgr A*. Phys. Rev. D **106**, 084051 (2022). https://doi.org/10.1103/PhysRevD.106.084051. arXiv:2207.09003

24. H. Falcke, F. Melia, E. Agol, Viewing the shadow of the black hole at the galactic center. Astrophys. J. Lett. **528**, L13 (2000). https://doi.org/10.1086/312423. arXiv:astro-ph/9912263

25. Z. Xu, X. Hou, J. Wang, Possibility of Identifying Matter around Rotating Black Hole with Black Hole Shadow. JCAP **10**, 046 (2018). https://doi.org/10.1088/1475-7516/2018/10/046. arXiv:1806.09415

26. X. Hou, Z. Xu, M. Zhou, J. Wang, Black hole shadow of Sgr A* in dark matter halo. JCAP **07**, 015 (2018). https://doi.org/10.1088/1475-7516/2018/07/015. arXiv:1804.08110

27. X. Hou, Z. Xu, J. Wang, Rotating Black Hole Shadow in Perfect Fluid Dark Matter. JCAP **12**, 040 (2018). https://doi.org/10.1088/1475-7516/2018/12/040. arXiv:1810.06381

28. M. Okyay, A. Övgün, Nonlinear electrodynamics effects on the black hole shadow, deflection angle, quasinormal modes and greybody factors. JCAP **01**, 009 (2022). https://doi.org/10.1088/1475-7516/2022/01/009. arXiv:2108.07766

29. Y. Yang, D. Liu, A. Övgün, Z.-W. Long, G. Lambiase, Rotating black bounces surrounded by the string cloud, arXiv:2307.09344

30. Y. Kumaran, A. Övgün, Shadow and deflection angle of asymptotic, magnetically-charged, non-singular black hole. arXiv:2306.04705

31. G. Lambiase, R.C. Pantig, D.J. Gogoi, A. Övgün, Investigating the connection between generalized uncertainty principle and asymptotically safe gravity in black hole signatures through shadow and quasinormal modes. Eur. Phys. J. C **83**, 679 (2023). https://doi.org/10.1140/epjc/s10052-023-11848-6. arXiv:2304.00183

32. A. Uniyal, R.C. Pantig, A. Övgün, Probing a non-linear electrodynamics black hole with thin accretion disk, shadow, and deflection angle with M87* and Sgr A* from EHT. Phys. Dark Univ. **40**, 101178 (2023). https://doi.org/10.1016/j.dark.2023.101178. arXiv:2205.11072

33. A. Uniyal, S. Chakrabarti, R.C. Pantig, A. Övgün, Nonlinearly charged black holes: Shadow and Thin-accretion disk. arXiv:2303.07174

34. A. Övgün, R.C. Pantig, A. Rincón, 4D scale-dependent Schwarzschild-AdS/dS black holes: study of shadow and weak deflection angle and greybody bounding. Eur. Phys. J. Plus **138**, 192 (2023). https://doi.org/10.1140/epjp/s13360-023-03793-w. arXiv:2303.01696

35. F. Atamurotov, I. Hussain, G. Mustafa, A. Övgün, Weak deflection angle and shadow cast by the charged-Kiselev black hole with cloud of strings in plasma*. Chin. Phys. C **47**, 025102 (2023). https://doi.org/10.1088/1674-1137/ac9fbb

36. Y. Kumaran, A. Övgün, Deflection Angle and Shadow of the Reissner-Nordström Black Hole with Higher-Order Magnetic Correction in Einstein-Nonlinear-Maxwell Fields. Symmetry **14**, 2054 (2022). https://doi.org/10.3390/sym14102054. arXiv:2210.00468

37. R.C. Pantig, A. Övgün, D. Demir, Testing symmergent gravity through the shadow image and weak field photon deflection by a rotating black hole using the M87* *and Sgr. A* results*. Eur. Phys. J. C **83**, 250 (2023). https://doi.org/10.1140/epjc/s10052-023-11400-6. arXiv:2208.02969

38. G. Mustafa, F. Atamurotov, I. Hussain, S. Shaymatov, A. Övgün, Shadows and gravitational weak lensing by the Schwarzschild black hole in the string cloud background with quintessential field*. Chin. Phys. C **46**, 125107 (2022). https://doi.org/10.1088/1674-1137/ac917f. arXiv:2207.07608

39. J. Rayimbaev, R.C. Pantig, A. Övgün, A. Abdujabbarov, D. Demir, Quasiperiodic oscillations, weak field lensing and shadow cast around black holes in Symmergent gravity. Annals Phys. **454**, 169335 (2023). https://doi.org/10.1016/j.aop.2023.169335. arXiv:2206.06599

40. R.C. Pantig, A. Övgün, Testing dynamical torsion effects on the charged black hole's shadow, deflection angle and greybody with M87* and Sgr. A* from EHT. Annals Phys. **448**, 169197 (2023). https://doi.org/10.1016/j.aop.2022.169197. arXiv:2206.02161

41. L. Chakhchi, H. El Moumni, K. Masmar, Shadows and optical appearance of a power-Yang-Mills black hole surrounded by different accretion disk profiles. Phys. Rev. D **105**, 064031 (2022). https://doi.org/10.1103/PhysRevD.105.064031

42. X.-M. Kuang, A. Övgün, Strong gravitational lensing and shadow constraint from M87* of slowly rotating Kerr-like black hole. Ann. Phys. **447**, 169147 (2022). https://doi.org/10.1016/j.aop.2022.169147. arXiv:2205.11003

43. I. Çimdiker, D. Demir, A. Övgün, Black hole shadow in symmergent gravity. Phys. Dark Univ. **34**, 100900 (2021). https://doi.org/10.1016/j.dark.2021.100900. arXiv:2110.11904

44. I. I. Cimdiker, A. Övgün, D. Durmus, Thin accretion disk images of the black hole in symmergent gravity. Class. Quantum Grav. **40** (2023). https://doi.org/10.1088/1361-6382/aceb45

45. N. Tsukamoto, Z. Li, C. Bambi, Constraining the spin and the deformation parameters from the black hole shadow. JCAP **06**, 043 (2014). https://doi.org/10.1088/1475-7516/2014/06/043. arXiv:1403.0371

46. N. Tsukamoto, Black hole shadow in an asymptotically-flat, stationary, and axisymmetric spacetime: The Kerr-Newman and rotating regular black holes. Phys. Rev. D **97**, 064021 (2018). https://doi.org/10.1103/PhysRevD.97.064021. arXiv:1708.07427

47. R. Shaikh, Black hole shadow in a general rotating spacetime obtained through Newman-Janis algorithm. Phys. Rev. D **100**, 024028 (2019). https://doi.org/10.1103/PhysRevD.100.024028. arXiv:1904.08322

48. R. Shaikh, Shadows of rotating wormholes. Phys. Rev. D **98**, 024044 (2018). https://doi.org/10.1103/PhysRevD.98.024044. arXiv:1803.11422

49. S. Kasuya, M. Kobayashi, Throat effects on shadows of Kerr-like wormholes. Phys. Rev. D **103**, 104050 (2021). https://doi.org/10.1103/PhysRevD.103.104050. arXiv:2103.13086

50. A. Övgün, I. Sakallı, J. Saavedra, Shadow cast and Deflection angle of Kerr-Newman-Kasuya spacetime. JCAP **10**, 041 (2018). https://doi.org/10.1088/1475-7516/2018/10/041. arXiv:1807.00388

51. M. Fathi, M. Olivares, J.R. Villanueva, Spherical photon orbits around a rotating black hole with quintessence and cloud of strings. Eur. Phys. J. Plus **138**, 7 (2023). https://doi.org/10.1140/epjp/s13360-022-03538-1. arXiv:2207.04076

52. A. Belhaj, M. Benali, A.E. Balali, W.E. Hadri, H. El Moumni, Cosmological constant effect on charged and rotating black hole shadows. Int. J. Geom. Meth. Mod. Phys. **18**, 2150188 (2021). https://doi.org/10.1142/S0219887821501887. arXiv:2007.09058

53. A. Belhaj, H. Belmahi, M. Benali, W. El Hadri, H. El Moumni, E. Torrente-Lujan, Shadows of 5D black holes from string theory. Phys. Lett. B **812**, 136025 (2021). https://doi.org/10.1016/j.physletb.2020.136025. arXiv:2008.13478

54. S. Vagnozzi, R. Roy, Y.-D. Tsai, L. Visinelli, M. Afrin, A. Allahyari et al., Horizon-scale tests of gravity theories and fundamental physics from the event horizon telescope image of sagittarius a. Class. Quantum Gravity **40**, 165007 (2023). https://doi.org/10.1088/1361-6382/acd97b

55. Y. Chen, R. Roy, S. Vagnozzi, L. Visinelli, Superradiant evolution of the shadow and photon ring of Sgr A⋆. Phys. Rev. D **106**, 043021 (2022). https://doi.org/10.1103/PhysRevD.106.043021. arXiv:2205.06238

56. R. Roy, S. Vagnozzi, L. Visinelli, Superradiance evolution of black hole shadows revisited. Phys. Rev. D **105**, 083002 (2022). https://doi.org/10.1103/PhysRevD.105.083002. arXiv:2112.06932

57. S. Vagnozzi, C. Bambi, L. Visinelli, Concerns regarding the use of black hole shadows as standard rulers. Class. Quant. Grav. **37**, 087001 (2020). https://doi.org/10.1088/1361-6382/ab7965. arXiv:2001.02986

58. C. Bambi, K. Freese, Apparent shape of super-spinning black holes. Phys. Rev. D **79**, 043002 (2009). https://doi.org/10.1103/PhysRevD.79.043002. arXiv:0812.1328

59. C. Bambi, K. Freese, S. Vagnozzi, L. Visinelli, Testing the rotational nature of the supermassive object M87* from the circularity and size of its first image. Phys. Rev. D **100**, 044057 (2019). https://doi.org/10.1103/PhysRevD.100.044057. arXiv:1904.12983

60. C. Bambi, N. Yoshida, Shape and position of the shadow in the $\delta = 2$ Tomimatsu-Sato space-time. Class. Quant. Grav. **27**, 205006 (2010). https://doi.org/10.1088/0264-9381/27/20/205006. arXiv:1004.3149

61. A.F. Zakharov, Constraints on a charge in the Reissner-Nordström metric for the black hole at the Galactic Center. Phys. Rev. D **90**, 062007 (2014). https://doi.org/10.1103/PhysRevD.90.062007. arXiv:1407.7457

62. A.F. Zakharov, F. De Paolis, G. Ingrosso, A.A. Nucita, Direct Measurements of Black Hole Charge with Future Astrometrical Missions. Astron. Astrophys. **442**, 795 (2005). https://doi.org/10.1051/0004-6361:20053432. arXiv:astro-ph/0505286

63. A.F. Zakharov, F. De Paolis, G. Ingrosso, A.A. Nucita, Shadows as a tool to evaluate black hole parameters and a dimension of spacetime. New Astron. Rev. **56**, 64 (2012). https://doi.org/10.1016/j.newar.2011.09.002

64. A.F. Zakharov, The black hole at the Galactic Center: observations and models. Int. J. Mod. Phys. D **27**, 1841009 (2018). https://doi.org/10.1142/S0218271818410092. arXiv:1801.09920

65. A.F. Zakharov, Constraints on a Tidal Charge of the Supermassive Black Hole in M87* with the EHT Observations in April 2017. Universe **8**, 141 (2022). https://doi.org/10.3390/universe8030141. arXiv:2108.01533

66. R. Kumar Walia, S.G. Ghosh, S.D. Maharaj, Testing Rotating Regular Metrics with EHT Results of Sgr A*. Astrophys. J. **939**, 77 (2022). https://doi.org/10.3847/1538-4357/ac9623. arXiv:2207.00078

67. R.A. Konoplya, A. Zhidenko, Shadows of parametrized axially symmetric black holes allowing for separation of variables. Phys. Rev. D **103**, 104033 (2021). https://doi.org/10.1103/PhysRevD.103.104033. arXiv:2103.03855

68. M. Khodadi, G. Lambiase, D.F. Mota, No-hair theorem in the wake of Event Horizon Telescope. JCAP **09**, 028 (2021). https://doi.org/10.1088/1475-7516/2021/09/028. arXiv:2107.00834

69. M. Khodadi, G. Lambiase, Probing Lorentz symmetry violation using the first image of Sagittarius A*: Constraints on standard-model extension coefficients. Phys. Rev. D **106**, 104050 (2022). https://doi.org/10.1103/PhysRevD.106.104050. arXiv:2206.08601

70. R.C. Pantig, A. Övgün, Black Hole in Quantum Wave Dark Matter. Fortsch. Phys. **71**, 2200164 (2023). https://doi.org/10.1002/prop.202200164. arXiv:2210.00523

71. R.C. Pantig, A. Övgün, Dark matter effect on the weak deflection angle by black holes at the center of Milky Way and M87 galaxies. Eur. Phys. J. C **82**, 391 (2022). https://doi.org/10.1140/epjc/s10052-022-10319-8. arXiv:2201.03365

72. R.C. Pantig, P.K. Yu, E.T. Rodulfo, A. Övgün, Shadow and weak deflection angle of extended uncertainty principle black hole surrounded with dark matter. Annals Phys. **436**, 168722 (2022). https://doi.org/10.1016/j.aop.2021.168722. arXiv:2104.04304

73. R.C. Pantig, A. Övgün, Dehnen halo effect on a black hole in an ultra-faint dwarf galaxy. JCAP **08**, 056 (2022). https://doi.org/10.1088/1475-7516/2022/08/056. arXiv:2202.07404

74. S. Nampalliwar, S. Kumar, K. Jusufi, Q. Wu, M. Jamil, P. Salucci, Modeling the Sgr A* Black Hole Immersed in a Dark Matter Spike. Astrophys. J. **916**, 116 (2021). https://doi.org/10.3847/1538-4357/ac05cc. arXiv:2103.12439

75. S.V.M.C.B. Xavier, H.C.D. Lima, Junior., L.C.B. Crispino, Shadows of black holes with dark matter halo. Phys. Rev. D **107**, 064040 (2023). https://doi.org/10.1103/PhysRevD.107.064040. arXiv:2303.17666

76. N. Parbin, D.J. Gogoi, U.D. Goswami, Weak gravitational lensing and shadow cast by rotating black holes in axionic Chern-Simons theory. Phys. Dark Univ. **41**, 101265 (2023). https://doi.org/10.1016/j.dark.2023.101265. arXiv:2305.09157

77. G. Mustafa, F. Atamurotov, S.G. Ghosh, Structural properties of generalized embedded wormhole solutions via dark matter halos in Einsteinian-cubic-gravity with quasi-periodic oscillations. Phys. Dark Univ. **40**, 101214 (2023). https://doi.org/10.1016/j.dark.2023.101214

78. S. Capozziello, S. Zare, D. Mota, H. Hassanabadi, Dark matter spike around bumblebee black holes. JCAP **2023**, 027 (2023). https://doi.org/10.1088/1475-7516/2023/05/027. arXiv:2303.13554

79. X. Qin, S. Chen, Z. Zhang, J. Jing, Polarized image of a rotating black hole surrounded by a cold dark matter halo. Eur. Phys. J. C **83**, 159 (2023). https://doi.org/10.1140/epjc/s10052-023-11300-9. arXiv:2301.01551

80. G. Mustafa, S.K. Maurya, S. Ray, On the possibility of generalized wormhole formation in the galactic halo due to dark matter using the observational data within the matter coupling gravity formalism. Astrophys. J. **941**, 170 (2022). https://doi.org/10.3847/1538-4357/ac9b00

81. D. Pugliese, Z. Stuchlík, Dark matter effect on black hole accretion disks. Phys. Rev. D **106**, 124034 (2022). https://doi.org/10.1103/PhysRevD.106.124034

82. R.A. Konoplya, A. Zhidenko, Solutions of the Einstein Equations for a Black Hole Surrounded by a Galactic Halo. Astrophys.

J. **933**, 166 (2022). https://doi.org/10.3847/1538-4357/ac76bc. arXiv:2202.02205

83. R.A. Konoplya, Shadow of a black hole surrounded by dark matter. Phys. Lett. B **795**, 1 (2019). https://doi.org/10.1016/j.physletb.2019.05.043. arXiv:1905.00064

84. L.S. Bhandari, A.M. Thalapillil, Exploring millicharged dark matter components from the shadows. JCAP **03**, 043 (2022). https://doi.org/10.1088/1475-7516/2022/03/043. arXiv:2112.13858

85. C. Zhang, T. Zhu, A. Wang, Gravitational axial perturbations of Schwarzschild-like black holes in dark matter halos. Phys. Rev. D **104**, 124082 (2021). https://doi.org/10.1103/PhysRevD.104.124082. arXiv:2111.04966

86. K. Saurabh, K. Jusufi, Imprints of dark matter on black hole shadows using spherical accretions. Eur. Phys. J. C **81**, 490 (2021). https://doi.org/10.1140/epjc/s10052-021-09280-9. arXiv:2009.10599

87. E. Contreras, A. Rincón, G. Panotopoulos, P. Bargueño, Geodesic analysis and black hole shadows on a general non-extremal rotating black hole in five-dimensional gauged supergravity. Ann. Phys. **432**, 168567 (2021). https://doi.org/10.1016/j.aop.2021.168567. arXiv:2010.03734

88. E. Contreras, A. Rincón, G. Panotopoulos, P. Bargueño, B. Koch, Black hole shadow of a rotating scale-dependent black hole. Phys. Rev. D **101**, 064053 (2020). https://doi.org/10.1103/PhysRevD.101.064053. arXiv:1906.06990

89. E. Contreras, J.M. Ramirez-Velasquez, A. Rincón, G. Panotopoulos, P. Bargueño, Black hole shadow of a rotating polytropic black hole by the Newman-Janis algorithm without complexification. Eur. Phys. J. C **79**, 802 (2019). https://doi.org/10.1140/epjc/s10052-019-7309-z. arXiv:1905.11443

90. C.A.R. Herdeiro, A.M. Pombo, E. Radu, P.V.P. Cunha, N. Sanchis-Gual, The imitation game: Proca stars that can mimic the Schwarzschild shadow. JCAP **04**, 051 (2021). https://doi.org/10.1088/1475-7516/2021/04/051. arXiv:2102.01703

91. I. Sengo, P.V.P. Cunha, C.A.R. Herdeiro, E. Radu, Kerr black holes with synchronised Proca hair: lensing, shadows and EHT constraints. JCAP **01**, 047 (2023). https://doi.org/10.1088/1475-7516/2023/01/047. arXiv:2209.06237

92. H.C.D.L. Junior, J.-Z. Yang, L.C.B. Crispino, P.V.P. Cunha, C.A.R. Herdeiro, Einstein-Maxwell-dilaton neutral black holes in strong magnetic fields: Topological charge, shadows, and lensing. Phys. Rev. D **105**, 064070 (2022). https://doi.org/10.1103/PhysRevD.105.064070. arXiv:2112.10802

93. H.C.D.L. Junior, P.V.P. Cunha, C.A.R. Herdeiro, L.C.B. Crispino, Shadows and lensing of black holes immersed in strong magnetic fields. Phys. Rev. D **104**, 044018 (2021). https://doi.org/10.1103/PhysRevD.104.044018. arXiv:2104.09577

94. H.C.D. Lima, Junior., L.C.B. Crispino, P.V.P. Cunha, C.A.R. Herdeiro, Can different black holes cast the same shadow? Phys. Rev. D **103**, 084040 (2021). https://doi.org/10.1103/PhysRevD.103.084040. arXiv:2102.07034

95. P.V.P. Cunha, C.A.R. Herdeiro, M.J. Rodriguez, Shadows of Exact Binary Black Holes. Phys. Rev. D **98**, 044053 (2018). https://doi.org/10.1103/PhysRevD.98.044053. arXiv:1805.03798

96. P.V.P. Cunha, C.A.R. Herdeiro, M.J. Rodriguez, Does the black hole shadow probe the event horizon geometry? Phys. Rev. D **97**, 084020 (2018). https://doi.org/10.1103/PhysRevD.97.084020. arXiv:1802.02675

97. P.V.P. Cunha, C.A.R. Herdeiro, E. Radu, H.F. Runarsson, Shadows of Kerr black holes with scalar hair. Phys. Rev. Lett. **115**, 211102 (2015). https://doi.org/10.1103/PhysRevLett.115.211102. arXiv:1509.00021

98. M. Guerrero, G.J. Olmo, D. Rubiera-Garcia, D.S.-C. Gómez, Shadows and optical appearance of black bounces illuminated by a thin accretion disk. JCAP **08**, 036 (2021). https://doi.org/10.1088/1475-7516/2021/08/036. arXiv:2105.15073

99. M. Guerrero, G.J. Olmo, D. Rubiera-Garcia, Double shadows of reflection-asymmetric wormholes supported by positive energy thin-shells. JCAP **04**, 066 (2021). https://doi.org/10.1088/1475-7516/2021/04/066. arXiv:2102.00840

100. M. Sharif, S. Iftikhar, Shadow of a charged rotating non-commutative black hole. Eur. Phys. J. C **76**, 630 (2016). https://doi.org/10.1140/epjc/s10052-016-4472-3. arXiv:1611.00611

101. M. Amir, K. Jusufi, A. Banerjee, S. Hansraj, Shadow images of Kerr-like wormholes. Class. Quant. Grav. **36**, 215007 (2019). https://doi.org/10.1088/1361-6382/ab42be. arXiv:1806.07782

102. M. Khodadi, Shadow of black hole surrounded by magnetized plasma: Axion-plasmon cloud. Nucl. Phys. B **985**, 116014 (2022). https://doi.org/10.1016/j.nuclphysb.2022.116014. arXiv:2211.00300

103. Y. Meng, X.-M. Kuang, X.-J. Wang, J.-P. Wu, Shadow revisiting and weak gravitational lensing with Chern-Simons modification. Phys. Lett. B **841**, 137940 (2023). https://doi.org/10.1016/j.physletb.2023.137940. arXiv:2305.04210

104. X.-J. Wang, X.-M. Kuang, Y. Meng, B. Wang, J.-P. Wu, Rings and images of Horndeski hairy black hole illuminated by various thin accretions. Phys. Rev. D **107**, 124052 (2023). https://doi.org/10.1103/PhysRevD.107.124052. arXiv:2304.10015

105. Y.-Z. Li, X.-M. Kuang, Precession of bounded orbits and shadow in quantum black hole spacetime. Phys. Rev. D **107**, 064052 (2023). https://doi.org/10.1103/PhysRevD.107.064052

106. X.-M. Kuang, Z.-Y. Tang, B. Wang, A. Wang, Constraining a modified gravity theory in strong gravitational lensing and black hole shadow observations. Phys. Rev. D **106**, 064012 (2022). https://doi.org/10.1103/PhysRevD.106.064012. arXiv:2206.05878

107. Y. Meng, X.-M. Kuang, Z.-Y. Tang, Photon regions, shadow observables, and constraints from M87* of a charged rotating black hole. Phys. Rev. D **106**, 064006 (2022). https://doi.org/10.1103/PhysRevD.106.064006. arXiv:2204.00897

108. A. Anjum, M. Afrin, S.G. Ghosh, Investigating effects of dark matter on photon orbits and black hole shadows. Phys. Dark Univ. **40**, 101195 (2023). https://doi.org/10.1016/j.dark.2023.101195. arXiv:2301.06373

109. S.U. Islam, J. Kumar, R. Kumar Walia, S.G. Ghosh, Investigating Loop Quantum Gravity with Event Horizon Telescope Observations of the Effects of Rotating Black Holes. Astrophys. J. **943**, 22 (2023). https://doi.org/10.3847/1538-4357/aca411. arXiv:2211.06653

110. S.G. Ghosh, M. Afrin, An Upper Limit on the Charge of the Black Hole Sgr A* from EHT Observations. Astrophys. J. **944**, 174 (2023). https://doi.org/10.3847/1538-4357/acb695. arXiv:2206.02488

111. S.G. Ghosh, R. Kumar, S.U. Islam, Parameters estimation and strong gravitational lensing of nonsingular Kerr-Sen black holes. JCAP **03**, 056 (2021). https://doi.org/10.1088/1475-7516/2021/03/056. arXiv:2011.08023

112. A. Abdujabbarov, M. Amir, B. Ahmedov, S.G. Ghosh, Shadow of rotating regular black holes. Phys. Rev. D **93**, 104004 (2016). https://doi.org/10.1103/PhysRevD.93.104004. arXiv:1604.03809

113. R. Kumar, S.G. Ghosh, Rotating black holes in 4*D* Einstein-Gauss-Bonnet gravity and its shadow. JCAP **07**, 053 (2020). https://doi.org/10.1088/1475-7516/2020/07/053. arXiv:2003.08927

114. U. Papnoi, F. Atamurotov, S.G. Ghosh, B. Ahmedov, Shadow of five-dimensional rotating Myers-Perry black hole. Phys. Rev. D **90**, 024073 (2014). https://doi.org/10.1103/PhysRevD.90.024073. arXiv:1407.0834

115. R. Kumar, S.G. Ghosh, Black Hole Parameter Estimation from Its Shadow. Astrophys. J. **892**, 78 (2020). https://doi.org/10.3847/1538-4357/ab77b0. arXiv:1811.01260

116. B. Toshmatov, B. Ahmedov, A. Abdujabbarov, Z. Stuchlik, Rotating Regular Black Hole Solution. Phys. Rev. D **89**, 104017 (2014). https://doi.org/10.1103/PhysRevD.89.104017. arXiv:1404.6443

117. F. Atamurotov, A. Abdujabbarov, B. Ahmedov, Shadow of rotating non-Kerr black hole. Phys. Rev. D **88**, 064004 (2013). https://doi.org/10.1103/PhysRevD.88.064004

118. A.A. Abdujabbarov, L. Rezzolla, B.J. Ahmedov, A coordinate-independent characterization of a black hole shadow. Mon. Not. Roy. Astron. Soc. **454**, 2423 (2015). https://doi.org/10.1093/mnras/stv2079. arXiv:1503.09054

119. F. Atamurotov, B. Ahmedov, Optical properties of black hole in the presence of plasma: shadow. Phys. Rev. D **92**, 084005 (2015). https://doi.org/10.1103/PhysRevD.92.084005. arXiv:1507.08131

120. M. Tang Z. Xu, The no-hair theorem and black hole shadows. JHEP **12**, 125 (2022). https://doi.org/10.1007/JHEP12(2022)125. arXiv:2209.08202

121. K.G. Begeman, A.H. Broeils, R.H. Sanders, Extended rotation curves of spiral galaxies: Dark haloes and modified dynamics. Mon. Not. Roy. Astron. Soc. **249**, 523 (1991). https://doi.org/10.1093/mnras/249.3.523

122. Z. Xu, X. Hou, X. Gong, J. Wang, Black Hole Space-time In Dark Matter Halo. JCAP **09**, 038 (2018). https://doi.org/10.1088/1475-7516/2018/09/038. arXiv:1803.00767

123. Z. Xu, J. Wang, M. Tang, Deformed black hole immersed in dark matter spike. JCAP **09**, 007 (2021). https://doi.org/10.1088/1475-7516/2021/09/007. arXiv:2104.13158

124. T. Matos, D. Nunez, The general relativistic geometry of the Navarro - Frenk - White model. Rev. Mex. Fis. Ser. **51**, 71 (2005). arXiv:astro-ph/0303594

125. H. Erbin, Janis-Newman algorithm: generating rotating and NUT charged black holes. Universe **3**, 19 (2017). https://doi.org/10.3390/universe3010019. arXiv:1701.00037

126. M. Azreg-Aïnou, Generating rotating regular black hole solutions without complexification. Phys. Rev. D **90**, 064041 (2014). https://doi.org/10.1103/PhysRevD.90.064041. arXiv:1405.2569

127. B. Carter, Global structure of the Kerr family of gravitational fields. Phys. Rev. **174**, 1559 (1968). https://doi.org/10.1103/PhysRev.174.1559

128. T. Johannsen, Photon Rings around Kerr and Kerr-like Black Holes. Astrophys. J. **777**, 170 (2013). https://doi.org/10.1088/0004-637X/777/2/170. arXiv:1501.02814

129. K. Hioki, K.-I. Maeda, Measurement of the Kerr Spin Parameter by Observation of a Compact Object's Shadow. Phys. Rev. D **80**, 024042 (2009). https://doi.org/10.1103/PhysRevD.80.024042. arXiv:0904.3575